Spatial Interference: From Coherent to Incoherent

Su-Heng Zhang,[1] Lu Gao,[1] Jun Xiong,[1] Li-Juan Feng,[1] De-Zhong Cao,[2] and Kaige Wang[1,*]

[1]*Department of Physics, Applied Optics Beijing Area Major Laboratory, Beijing Normal University, Beijing 100875, China*
[2]*Department of Physics, Yantai University, Yantai 264005, China*

(Received 24 July 2008; revised manuscript received 16 January 2009; published 20 February 2009)

We report an optical interference experiment which seems to contradict our common knowledge, in that the formation of the interference pattern originates from a spatially incoherent light source. Our experimental scheme is very similar to Gabor's original proposal of holography [Nature (London) **161**, 777 (1948)], except that an incoherent source replaces the coherent one. Though an instantaneous interference pattern between an object wave and reference wave fluctuates irregularly, a well-defined pattern appears in the statistical average, in accord with a hologram in the coherent light case.

DOI: 10.1103/PhysRevLett.102.073904 PACS numbers: 42.25.Kb, 42.25.Hz, 42.40.Kw

In the early days when coherent sources were unavailable, interference experiments were carried out with a thermal light source and the help of a pinhole aperture. Though the latter can improve the spatial coherence of the source, it substantially reduces the power of the source and thus restricts the practical applications of optical interferometric techniques such as holography. Later, efforts to realize interference with chaotic light began after the landmark experiment of Hanbury Brown and Twiss [1] who realized that light from different, completely uncorrelated portions of a star gives rise to an interference effect, which is visible in the intensity correlations but not in the intensities themselves, and proposed an intensity interferometer to measure the angular size of distant stars. The interference related to the intensity correlation property of spatially incoherent light has since been clearly demonstrated in ghost interference and subwavelength interference experiments [2–8]. The complementarity between the coherence of the beams and the ability of performing ghost imaging has been discussed in Refs. [9,10]. The physics behind these effects is that each point of a spatially incoherent source produces coherence of the field at two separate positions, after having travelled different paths, and the coherence information can be acquired through an intensity correlation measurement at the two positions. Moreover, Ref. [11] reported that the phase and amplitude of the field correlation function of the two positions can be retrieved by a modified Young's interferometer, instead of through intensity correlation measurements. However, there is still a challenging question of whether, with an incoherent light source, the coherence information can be recorded through just the intensity distribution itself.

In this Letter, we propose a scenario which is capable of observing interference and diffraction with a spatially incoherent source solely through intensity measurements. The experimental setups of the interferometer are sketched in Fig. 1, and are similar to Gabor's original proposal of holography. The source field beam is divided into two parts: one illuminates an object, called the object wave, and the other acts as a reference wave. Interference occurs at the outgoing beam splitter BS_2 and the fringes can be recorded by either of two CCD cameras. The interference terms of the fields at the two outgoing ports have a phase shift π due to the reflection and transmission at the beam splitter. The object in the experiments is a double slit of slit width $b = 125\ \mu$m and spacing $d = 310\ \mu$m. As a proof-of-principle experiment, we first use a pseudothermal light source, which is formed by passing a He-Ne laser beam of wavelength 632.8 nm through a ground glass disk G rotating slowly at 0.002 Hz. The CCD cameras register each frame of the interference pattern with an exposure time of 40 ms. The pattern fluctuates randomly as the ground glass

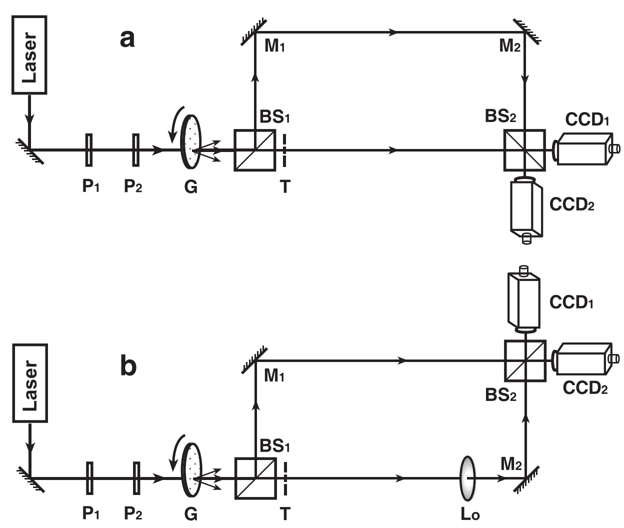

FIG. 1. Experimental schemes for an unbalanced interferometer using an incoherent light source. P_1 and P_2 are two polarizers for modulating the intensity; G is a rotating ground glass disk; CCD_1 and CCD_2 are two CCD cameras. Two mirrors, M_1 and M_2, and two beam splitters, BS_1 and BS_2, form an interferometer. The object T is a double slit close to BS_1. (a) The two arms have different lengths; (b) A lens L_o of focal length f_o is set in the middle of the object arm, and both arms have the same length $2f_o$.

rotates. We first consider the scheme of Fig. 1(a) in which the two waves travel different distances: $z_o = 16$ cm for the object wave and $z_r = 27$ cm for the reference wave, and $|z_o - z_r|/c$ is less than the coherence time of the laser beam. The two-dimensional (2D) intensity patterns detected by CCD_1 are shown in Fig. 2. We can see that a single-shot frame in Fig. 2(a) shows an irregular pattern. However, if we average over a number of exposures, as the number of frames increases, a well-defined interference pattern emerges gradually, as can be seen in Figs. 2(b) and 2(c).

The above experimental results can be readily explained by fundamental optics theory. Let $E_o(x)$ and $E_r(x)$ be the object and reference fields at the recording plane, respectively. The propagation of the mutual co herence of the beams in the interferometer is given by [12] $\langle E_r^*(x_1)E_o(x_2)\rangle = \alpha_r^*\alpha_o \int h_r^*(x_1, x_0')T(x_0)h_o(x_2, x_0) \times \langle E_s^*(x_0')E_s(x_0)\rangle dx_0 dx_0'$, where $E_s(x_0)$ is the source field at beam splitter BS_1; $h_j(x, x_0)$ and α_j are the impulse response function between $E_s(x_0)$ and $E_j(x)$ ($j = o, r$), and the attenuation constant in each path, respectively; x_0 and x_j are the transverse positions across the beams. A transmittance object $T(x)$ is located close to BS_1 in the object path. However, the interference term described by $\langle E_r^*(x)E_o(x)\rangle$ can be observed in the outgoing intensity pattern of the interferometer. For a coherent source which is assumed to have a stationary plane wave front $\langle E_s^*(x_0')E_s(x_0)\rangle = E_s^*E_s$, the interference term is $\langle E_r^*(x)E_o(x)\rangle \propto \int T(x_0)h_o(x, x_0)dx_0$, where the reference field is separated and contributes as a constant. As for a chaotic source satisfying complete spatial incoherence $\langle E_s^*(x)E_s(x')\rangle = I_s\delta(x - x')$, the interference term is written as

$$\langle E_r^*(x)E_o(x)\rangle = \alpha_r^*\alpha_o I_s \int T(x_0)h_o(x, x_0)h_r^*(x, x_0)dx_0. \tag{1}$$

In comparison with the coherent light case, Eq. (1) describes diffraction in the joint object and reference paths.

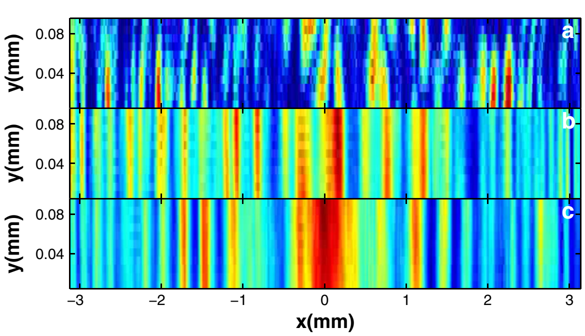

FIG. 2 (color online). Experimentally observed 2D interference patterns recorded by CCD_1 in the scheme of Fig. 1(a). (a) is an individual single frame; (b) and (c) are averaged over 100 and 10 000 frames, respectively.

But the conjugate wave front transfer in the reference path may counteract the diffraction in the object path. If both the object and reference waves travel in exactly the same configuration, i.e., $h_r = h_o$, as, for example, in a usual balanced interferometer, the diffraction has been completely eliminated and thus we observe the homogeneous distribution of the interference term. This used to be understood as an incoherent superposition effect which washes out the information of the object.

The fact that coherent information can be retained depends on whether $h_r^*(x, x_0)h_o(x, x_0)$ is an effective transfer function similar to $h_o(x, x_0)$. For this we modify the interferometer in an unbalanced way as shown in Fig. 1(a). For the moment, we assume that the source beam has temporal coherence, thus Eq. (1) is still valid when the path difference is such that $\langle E_s^*(x, t)E_s(x', t - |z_o - z_r|/c)\rangle \approx \langle E_s^*(x)E_s(x')\rangle$. In the paraxial propagation, the impulse response function for a length z is $H(x, x_0, z) \equiv \sqrt{k/(i2\pi z)}\exp(ikz)G(x - x_0, z)$, where $G(x, z) \equiv \exp[ikx^2/(2z)]$ is the quadratic phase factor which plays the central role in the diffraction, and k is the wave number of the beam. Using $H(x, x_0, z)$ in Eq. (1), we obtain

$$\begin{aligned}\langle E_r^*(x)E_o(x)\rangle &= \frac{\alpha_r^*\alpha_o I_s k}{2\pi\sqrt{z_o z_r}}\exp[ik(z_o - z_r)] \\ &\quad \times \int T(x_0)G(x - x_0, Z)dx_0 \\ &\approx (\alpha_r^*\alpha_o I_s k/\sqrt{2\pi z_o z_r}) \\ &\quad \times \exp[ik(z_o - z_r)]G(x, Z)\tilde{T}(kx/Z),\end{aligned} \tag{2}$$

where $G(x, z_o)G^*(x, z_r) = G(x, Z)$ when $Z = z_o z_r/(z_r - z_o)$ has been applied. Equation (2) represents the Fresnel diffraction integral of an object under the paraxial condition, and is the same as for a coherent source but with an effective object distance Z replacing the real one z_o. When the size of the object is much less than the area of the diffraction pattern, then the Fourier transform $\tilde{T}$ of object T can be deduced to be, for instance, $\tilde{T}(q) = (2b/\sqrt{2\pi})\text{sinc}(qb/2)\cos(qd/2)$ for the double slit.

In the above scheme, the interference occurs between different wave fronts of the source beam and demands good temporal coherence of the source, for instance, the coherence length is larger than $z_r - z_o = 11$ cm in the experiment. To release the requirement of temporal coherence, the two arms of the interferometer must have the same length, but this will cancel out the diffraction due to the conjugate correlation. The conflict can be resolved in the scheme of Fig. 1(b), in which the two arms of the interferometer have the same length but different diffraction configurations. A lens of focal length f_o is set in the middle of the object path of length $2f_o$ to give $h_o(x, x_0) = \sqrt{k/(i2\pi f_o)}\exp(2ikf_o)\exp(-ikxx_0/f_o)$. In this scheme, we obtain the interference term

$$\langle E_r^*(x)E_o(x)\rangle = \frac{\alpha_r^*\alpha_o I_s k}{2\sqrt{2}\pi f_o}\int T(x_0)G^*(x+x_0,2f_o)dx_0$$
$$\approx [\alpha_r^*\alpha_o I_s k/(2\sqrt{\pi}f_o)]G^*(x,2f_o)\tilde{T}[kx/(2f_o)]. \quad (3)$$

The experimental results of the present scheme with $f_o =$ 19 cm are shown in Fig. 3, where (a) and (b) are the average intensity patterns $\langle I_1(x)\rangle$ and $\langle I_2(x)\rangle$ with the fringe visibilities of 29% and 25% registered by CCD_1 and CCD_2, respectively. We can see that the two interference patterns with a phase shift π are formed in the average of 10 000 frames, which matches with the theoretical simulation of Eq. (3), in addition to an intensity background. Moreover, for a 50/50 beam splitter BS_2, if one outgoing field is $[E_o(x) + E_r(x)]/\sqrt{2}$, the other should be $[E_o(x) - E_r(x)]/\sqrt{2}$. Taking the difference and sum of the two outgoing intensities gives, respectively, the net interference pattern and the intensity background, as shown in Figs. 3(c) and 3(d). As a matter of fact, the homogeneous intensity background in Fig. 3(d) verifies the incoherence of the source. To further confirm whether the interference pattern is related to the spatial incoherence, we may compare it with the result obtained in the same interferometer using coherent light. For this we simply remove the ground glass in Fig. 1(b). In this case, the interference pattern for the coherent field consists of two parts, $|\tilde{T}(kx/f_o)|^2$ and $\tilde{T}(kx/f_o)$ + c.c.. The corresponding experimental results are plotted in Fig. 4, where (a) and (b) show the stable intensity patterns $I_1(x)$ and $I_2(x)$ registered by CCD_1 and CCD_2, respectively. After eliminating the background intensity of each arm, the net interference pattern in Fig. 4(c) fits the formula $\tilde{T}(kx/f_o)$, which has a doubled spatial frequency with respect to that in Eq. (3) for the incoherent source. Therefore, in the same interferometer, both coherent and incoherent sources can be used to perform the

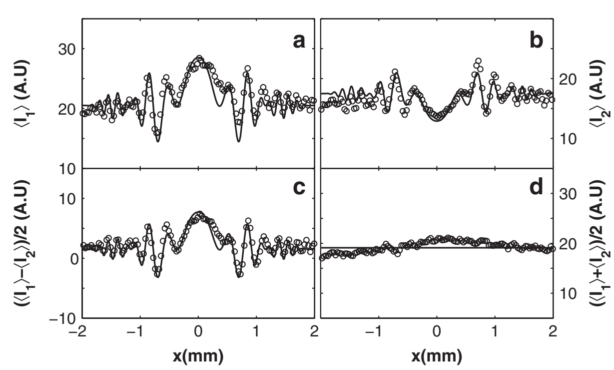

FIG. 3. Experimentally observed 1D interference patterns in the scheme of Fig. 1(b). (a, b) are interference patterns (averaged over 10 000 frames) registered by CCD_1 and CCD_2, respectively; (c, d) are their difference and summation, respectively. Experimental data and theoretical simulation are given by open circles and solid lines, respectively.

Fourier transform of an object but with different spatial frequencies.

To further demonstrate this effect, we must consider a true thermal light source. An extended quasimonochromatic thermal light source can be regarded as a spatially incoherent source with a short coherence time less than 0.1 nsec. Within the coherence time, the source can produce an instantaneous exposure of interference pattern in our schemes. Unlike with a pseudothermal light source, individual exposures cannot be registered directly by the slow CCD camera which has a response time on the order of milliseconds. Instead, an average intensity distribution of these exposures will appear on the CCD screen. We have indicated that the scheme of Fig. 1(b) is appropriate for observing interference using a true thermal light source, since the requirement of temporal coherence has been relaxed. We use a Na lamp of wavelength 589.3 nm with an illumination area of 10×10 mm^2 to replace the pseudothermal light source in Fig. 1(b), and find that the interference patterns with the visibility of 6.0% directly appear on the CCD screen, as shown in Fig. 5(b). For comparison, Fig. 5(a) shows the 2D interference pattern corresponding to Fig. 3(a) for pseudothermal light in the same interferometer. The fringes are similar, but with slightly different spacings, due to the different wavelengths of the two sources. Then we set a pinhole of diameter 0.36 mm after the lamp to dispel the spatial incoherence. With this pointlike source, a different interference pattern, which has half the fringe spacing of that for the spatially incoherent source, is recorded on the CCD screen, as shown in Fig. 5(c).

We note that the visibility of the interference fringes $(I_{max} - I_{min})/(I_{max} + I_{min})$ in the experiment is much better than that in ghost interference [3,8]. The visibility depends mainly on the spot size of the incident beam at BS_1 and the intensity ratio of the two interfering beams at the detection plane. A smaller input spot will increase the visibility, but is limited by the object size. Hence we obtain the maximum visibility when the spot impinging on BS_1 is taken as the size of the object while the intensities of two

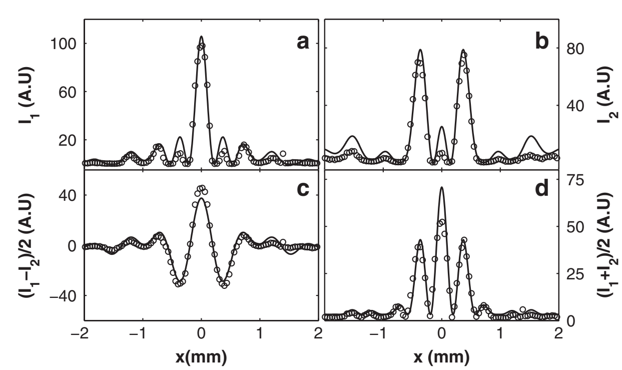

FIG. 4. Same as in Fig. 3 but with the ground glass disk in Fig. 1(b) removed. All the interference patterns are stable.

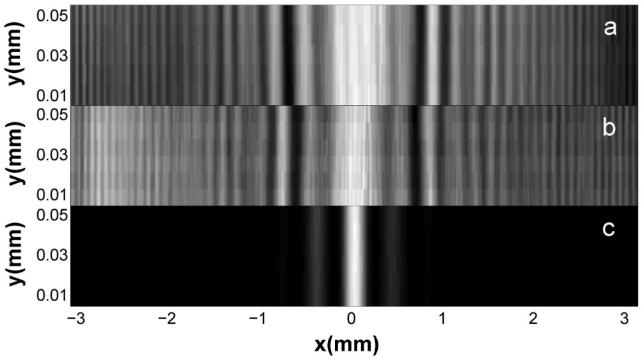

FIG. 5. Experimentally observed 2D interference patterns registered by CCD_1 in the scheme of Fig. 1(b): (a) with the original pseudothermal light source in Fig. 1(b), averaged over 10 000 frames; (b) with a Na lamp of extended illumination area as the light source; (c) with a Na lamp followed by a pinhole as the light source.

interfering beams are equal at BS_2. The theoretical simulation gives a maximum visibility of 58.9% for the scheme of Fig. 1(b) and 21.9% for the similar configuration of ghost interference. Similar to ghost imaging with thermal light, the visibility can be strongly enhanced by a posterior subtraction of the intensity background [through the difference of the two outgoing intensities, see Fig. 3(c)].

To conclude, we incorporate the transverse spatial correlation of a chaotic field into interferometry as incoherent interferometry to perform first-order interference. Physically, the interference in incoherent interferometry is based on the first-order spatial correlation of the chaotic field, similar in principle to ghost interference. Unlike in coherent interferometry, the diffraction is established through joint transfer of both object and reference fields where the latter behaves as the ‘‘conjugate and backward’’ action against the former [13]. Hence the effect cannot be observed in any common balanced interferometer. As soon as the diffraction balance in the two arms is broken, the interference pattern appearing in the statistical average is well defined in the manner of coherent interferometry. In comparison with ghost interference where the intensity correlation records the square modulus of interference distribution $|\tilde{T}(x)|^2$, the present scheme exhibits the net interference pattern $\tilde{T}(x)$ with a good visibility. However, the intensity measurement is much easier than the intensity correlation measurement, especially for high-frequency intensity fluctuations whose average can be recorded by low-frequency detection. These features are adequate for interference applications such as holography.

In the light of holography, our approach is fundamentally different from the previous method called ‘‘incoherent holography’’ [14]. In the latter, each source point in the object produces, by interfering its wave fronts, a stationary two-dimensional intensity pattern (e.g., Fresnel zone plate) which uniquely encodes the position and intensity of the object point, and hence the method is limited to recording only the intensity distribution of the fluorescent object. However, our approach records both amplitude and phase modulations about the object. With the relaxation of spatial coherence requirements, we may expect wider potential usage of the interference technology especially in those applications where a coherent source is unavailable, such as when x-ray and electron beams are required.

The authors thank L. A. Wu for helpful discussions. This work was supported by the National Fundamental Research Program of China, Project No. 2006CB921404, and the National Natural Science Foundation of China, Projects No. 10574015 and No. 10874019.

*Corresponding author.
wangkg@bnu.edu.cn

[1] R. Hanbury Brown and R. Q. Twiss, Nature (London) **178**, 1046 (1956).
[2] R. S. Bennink, S. J. Bentley, R. W. Boyd, and J. C. Howell, Phys. Rev. Lett. **92**, 033601 (2004).
[3] Y. Cai and S. Y. Zhu, Opt. Lett. **29**, 2716 (2004).
[4] K. Wang and D. Z. Cao, Phys. Rev. A **70**, 041801(R) (2004).
[5] G. Scarcelli, A. Valencia, and Y. Shih, Europhys. Lett. **68**, 618 (2004).
[6] F. Ferri *et al.*, Phys. Rev. Lett. **94**, 183602 (2005).
[7] J. Xiong *et al.*, Phys. Rev. Lett. **94**, 173601 (2005).
[8] Y. H. Zhai, X. H. Chen, D. Zhang, and L. A. Wu, Phys. Rev. A **72**, 043805 (2005).
[9] A. Gatti *et al.*, J. Mod. Opt. **53**, 739 (2006).
[10] M. Bache *et al.*, Phys. Rev. A **73**, 053802 (2006).
[11] R. Borghi, F. Gori, and M. Santarsiero, Phys. Rev. Lett. **96**, 183901 (2006).
[12] L. Mandel and E. Wolf, *Optical Coherence and Quantum Optics* (Cambrige University Press, Cambridge, England, 1995) p. 188.
[13] Spatial field correlation in an entangled photon pair exists between $E_1^{(-)}$ and $E_2^{(-)}$ [4]; Klyshko interpreted this in terms of ‘‘advanced wave interference’’: D. N. Klyshko, Phys. Lett. A **132**, 299 (1988).
[14] L. Mertz and N. O. Young, in *Proceedings of Conference on Optical Instruments and Techniques*, edited by K. J. Habell (Chapman and Hall, London, 1962); A. W. Lohmann, J. Opt. Soc. Am. **55**, 1555 (1965); G. Cochran, J. Opt. Soc. Am. **56**, 1513 (1966).